

Research Article

# Spatio-Temporal Variability and Trends of Annual and Seasonal Rainfall in Wolaita Zone, Ethiopia

Adujna Arba\* 

Ethiopian Meteorology Institute, SCSSW Regions Meteorological Service Research Center, Hawassa, Ethiopia

## Abstract

This paper examined the spatiotemporal variability and trends of rainfall in the Wolaita Zone, Ethiopia. Rainfall data from fifteen stations from 1991 to 2020 is included, as well as data from important stations with longer observation periods. The variability of rainfall at the annual and seasonal scales was analyzed by using the coefficient of variation (CV) and standardized rainfall anomalies (SRA) over the study area. Mann-Kendall test was used to determine trend and Sen's slope estimator was used to determine magnitude of the trend. Rainfall was highly variable during Belg season. The Belg season is the second rainy season, which received from 309.3 mm to 694.5 mm. Rainfall was moderately variable during the Kiremt season. The Kiremt season is the main rainy season, which received from 379.5 mm to 752.8 mm. Rainfall is less variable during annual times. At the annual time, rainfall was recorded from 910.3 mm to 1465.9 mm. At the annual and Kiremt time, almost all stations show increases in trend when P values < 0.005. On the other hand, at the Belg season, almost all stations show decreases in trends when P values < 0.005. The spatial distribution of rainfall is increasing in the highland area while decreasing in the lowland area of the Wolaita zone. The studying of rainfall variability and trend at temporal and spatial scales is hence useful for communities, local-level actors, and decision-makers for planning activities and devising appropriate adaptive strategies as well as to take informed decisions.

## Keywords

Mann-Kendall Test, Rainfall Variability, Sen's Slope, Wolaita Zone

## 1. Introduction

Rainfall is one of the most significant climate variables for global agricultural productivity [1]. It is a significant climate variability for East African countries, with extreme occurrences resulting in droughts and floods, which are often associated with food, energy, and water shortages; loss of life and property; and cause many other socio-economic impacts [2]. Unpredictable rainfall amounts and distribution behavior have become a congestion for agricultural and livestock production [3, 4]. Detailed analysis and quantification of

rainfall spatial distribution are required for water resource management, hydrological modeling, flood forecasting, and climate change studies [5].

Rainfall varies significantly in Ethiopia at both temporal and spatial scales. Most of the areas, more than 70% of the country, receive rainfall during the Kiremt season, extending from June to the end of September [6]. Spatially, the country is known for its diverse topography, including mountains, dissected plateaus, valleys, and plain lands or lowlands that

\*Corresponding author: [Aduarba143@gmail.com](mailto:Aduarba143@gmail.com) (Adujna Arba)

Received: 1 April 2025; Accepted: 23 April 2025; Published: 29 May 2025



Copyright: © The Author(s), 2025. Published by Science Publishing Group. This is an **Open Access** article, distributed under the terms of the Creative Commons Attribution 4.0 License (<http://creativecommons.org/licenses/by/4.0/>), which permits unrestricted use, distribution and reproduction in any medium, provided the original work is properly cited.

affect rainfall distribution [7]. Rainfall in the South Ethiopia Region varies significantly in amount, duration, and intensity. The variability and trend analysis of precipitation has obtained due attention, and many researchers have shown interest in this area due to its tremendous impact on both socio-economic and environmental challenges. Several studies on rainfall variability and trends have been conducted in Ethiopia.

Wolaita Zone, in southern parts of Ethiopia, has a high population density and is highly dependent on labor-intensive and small-scale agriculture. According to the Wolaita Zone Finance and Economic Development Department (WZFEDD), rainfall in the area varies greatly in terms of its distribution and amount, typically decreasing from highlands to lowlands [8]. In this area, earlier researchers have analyzed the effects of rainfall variability on household perceptions and its change in the Wolaita Zone [9]. Nevertheless, the analysis of the spatio-temporal variability and trends of seasonal and annual rainfall in the Wolaita zone has not been sufficiently investigated by other researchers. Therefore, this study analyzes and fills a gap by analyzing spatio-temporal variability and trends of seasonal and annual rainfall in the Wolaita Zone, south Ethiopia.

## 2. Materials and Methods

### 2.1. Description of the Study Area

Geographically, the Wolaita Zone is located between  $6.4^{\circ}$ - $7.1^{\circ}$ N and  $37.4^{\circ}$ - $38.2^{\circ}$ E. The Wolaita Zone is one of the zone administrations in southern Ethiopia. The Wolaita Zone is located southwest of Addis Ababa, following the tarmac road from Shashemane to Arba Minch. Alternatively, it is located 330 km southwest of Addis Ababa, following the tarmac road that passes through Hosanna to Arba Minch. Sodo is established at the foot of Mount Damota and currently serves as the capital city of the southern Ethiopian region and Wolaita Zone. Wolaita is bordered south by the Gamo Zone, west by the Omo River, which separates it from Dawro; northwest by the Kembata Zone and Tembaro Special Woreda; north by Hadiya; northeast by the Oromia Region; east by the Bilate River, which separates it from the Sidama Region; and southeast by Lake Abaya, which separates it from the Oromia Region, as shown in Figure 1.

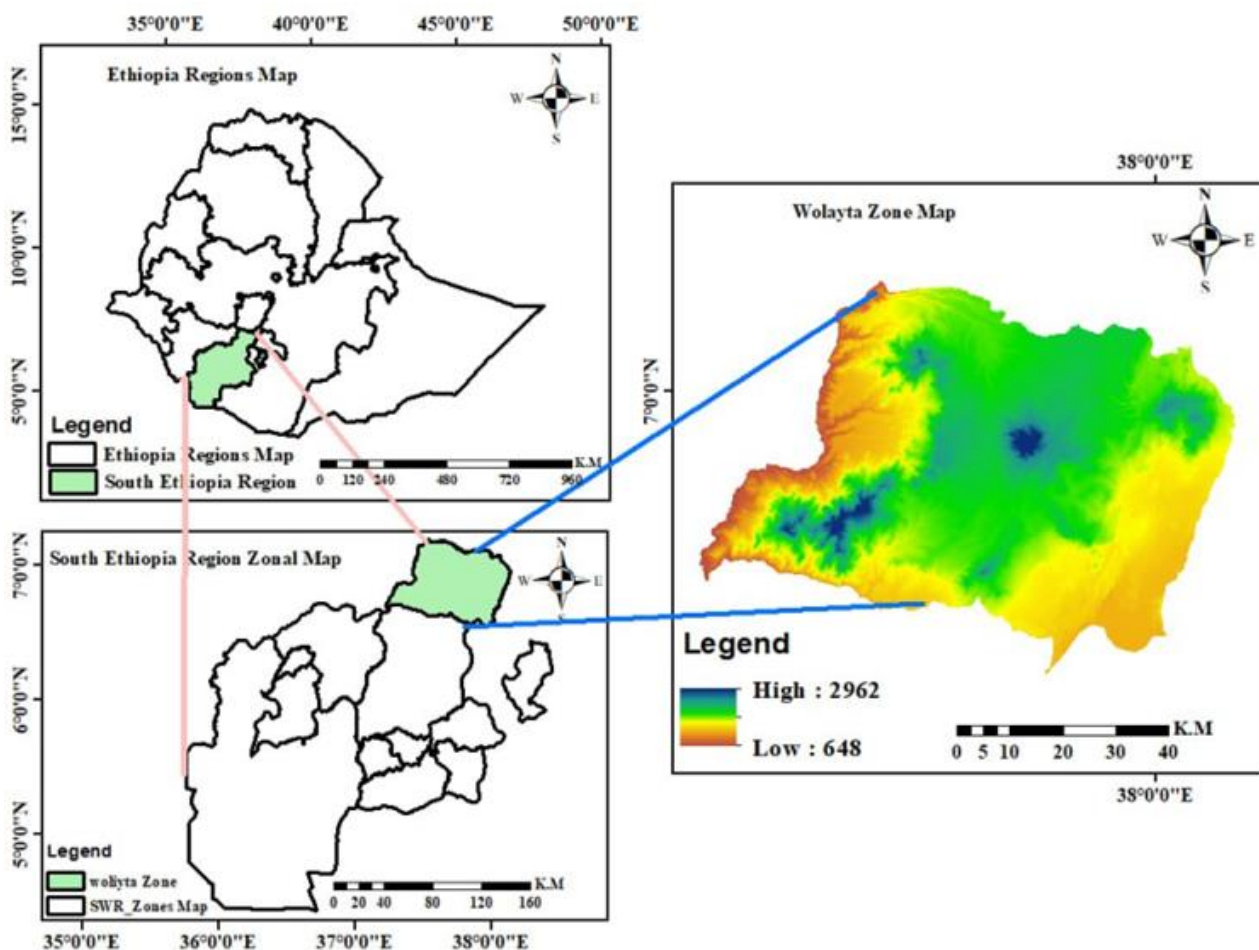


Figure 1. Study area map.

There are approximately 1,527,908 people living in the Wolaita zone, with men making up 49.3% of the population and women making up 51.7% [10]. The altitude ranges from 501 meters at Bilate-Tena to 3000 meters above sea level at Damota Mountain. The mean annual rainfall in the Wolaita Zone varies from 817.5 mm at Bilate-Tena to 1500.33 mm at Mayokote. There are three agro-ecological zones in the study area: Kolla, Woyna-Dega, and Dega. Each year, the average minimum and maximum temperatures are 15.5 °C and 24.5 °C, respectively. The rainfall distribution pattern is bimodal in the Wolaita Zone. The main rainy season, known as Kiremt, starts from mid-June to the end of September. The Belg season, also known as the short (secondary) rainy season, starts from mid-February to the end of May.

## 2.2. Data Types and Sources

The observed station data and grid data were collected from the Ethiopian Meteorology Institute (EMI). The stations for this study are selected on the basis of their representativeness within a given agro-ecology and the length of the recording period. To cover the study area, relatively long periods of rainfall data (1991-2020) with a reasonable geographical distribution from fifteen stations and daily gridded or Enhanced National Climate Services (ENACTS) rainfall data were used to fill in the missing data in this study. ENACTS is performed by improving the availability of timely, relevant and high-quality climate information at relevant spatiotemporal scales and working to promote the effective use of these data [11].

## 2.3. Methods

### 2.3.1. Variability Analysis

Coefficient of Variability (CV)

The coefficient of variation (CV) was used to analyze the annual and seasonal variability in rainfall via the following formula:

$$CV = \frac{\sigma}{x} * 100 \tag{1}$$

Where, CV = coefficient of variation,  $\sigma$  = standard deviation, and  $x$  = mean precipitation.

The coefficient of variation was used to categorize the amount of rainfall variability [12].

Accordingly, CV < 20 = less variable; CV 20-30 = moderately variable; and CV >30 = highly variable.

Standardized rainfall anomaly (SRA)

The variability of rainfall was computed via the standardized rainfall anomaly (SRA) method [13]. The standardized rainfall anomaly (SRA) was calculated as the difference between the annual total of a particular year and the long-term average rainfall records divided by the standard deviation of

the long-term data. This index is used to determine the inter-annual fluctuations in rainfall in the study area over the observation period and is represented mathematically as follows:

$$SRA = \frac{Pt - Pm}{\sigma} \tag{2}$$

Where, SRA is the standardized rainfall anomaly, Pt is the annual rainfall in year t, Pm is the long-term mean annual rainfall over the observation period, and  $\sigma$  is the standard deviation of the annual rainfall over the observation period. According to [14], the Z values are classified as extremely wet ( $Z > 2$ ), very wet ( $1.9 > Z > 1.5$ ), moderately wet ( $1.49 > Z > 1.0$ ), nearly normal ( $0.99 > Z > -0.99$ ), moderately dry ( $-1.0 > Z > -1.49$ ), severely dry ( $-1.5 > Z > -1.99$ ), or extremely dry ( $Z < -2$ ).

### 2.3.2. Trend Analysis

*Mann-Kendall test:* The Mann-Kendall (MK) statistic test [15, 16] is advised by the WMO for spotting trends in meteorological data [17]. This study applied the Mann-Kendall (MK) trend test method for historical and future rainfall data analysis via XLSTAT. A nonparametric technique called the Mann-Kendall (MK) test is used to identify trends in the time series of rainfall data. For non-normally distributed data series, such as rainfall data, the MK test is also recommended [18]. The seasonal and annual rainfall series were analyzed via the MK test. If the value in a time series is greater than its previous value, a score of +1 is given; conversely, a score of -1 is given. Let  $X_1, X_2, X_3, \dots, X_n$  represent n data points, where  $X_j$  represents the data point at time j. Then, the Mann-Kendall statistics (S) are given by

$$S = \sum_{i=1}^{n-1} \sum_{j=i+1}^n Sign(Xj - Xi) \tag{3}$$

Where, the sign function is:

$$Sign(Xj - Xi) = \begin{cases} +1 & Xj > Xi \\ 0 & Xj = Xi \\ -1 & Xj < Xi \end{cases} \tag{4}$$

Where,  $X_j$  and  $X_i$  are the sequential data values in months j and i ( $j > i$ ), respectively.

An increasing (upward) trend is shown by a positive value of S, whereas a decreasing (downward) trend is represented by a negative number. At the 0.01, 0.05, and 0.1 significance levels, the statistical significance of an increasing or decreasing trend in the mean precipitation and temperature values is assessed via a normalized test statistic (Z score).

$$z = \begin{cases} \frac{S-1}{\sqrt{\text{var}(s)}} S > 0 \\ 0 & S = 0 \\ \frac{S+1}{\sqrt{\text{var}(s)}} S < 0 \end{cases} \quad (5)$$

Where, the variance of S is calculated as

$$\text{Var}(s) = \frac{1}{18} [n(n-1)(2n+5) - \sum_{i=1}^g t_i(t_i-1)(2t_i+5)] \quad (6)$$

Where, g is the number of tied groups,  $t_i$  is the number of tied values in the  $i^{\text{th}}$  group,  $\text{Var}(S)$  is the reduction in the variance, and n is the number of data points.

This Z value and the Z value for (-1) from the standard normal distribution are compared to determine the significance.

Sen's slope estimator:

Sen's slope estimator was used to determine the trend magnitude at a specific time [19, 20]. Tests are frequently employed to measure the magnitude of a trend in time series rainfall data [21, 22]. The slope for all the data pairs can be calculated as follows:

$$T_i = \frac{x_j - x_i}{j - i} \text{ for } i = 1, 2, 3, \dots, N \quad (7)$$

Where,  $X_j$  and  $X_i$  are the data values at times j and i ( $j > i$ ), respectively. When there is one data point in each time period,  $N = \frac{n(n-1)}{2}$ , where n is the number of time periods. However, if there are more data points, then,  $N < \frac{n(n-1)}{2}$ , where, n is the total number of observations. The values of N are arranged from smallest to largest. The median of these "n" values of  $T_i$  is then represented by Sen's slope of estimation, which is calculated via the following equation:

$$Q_i = \begin{cases} \frac{T(N+1)}{2} \text{ for } N \text{ odd observations} \\ \frac{1}{2} \left( \frac{T(N)}{2} + \frac{T(N+1)}{2} \right) \text{ for } N \text{ even observation} \end{cases} \quad (8)$$

A positive value of  $Q_i$  indicates an increasing magnitude, and a negative value of  $Q_i$  represents a decreasing magnitude.

### 2.3.3. Analyzing Spatial Variation

Using the grid points at various time scales, surface data for rainfall was produced using ArcGIS's inverse distance weighted (IDW) interpolation approach. This was accomplished using the ArcGIS 10.8 interface to evaluate time series rainfall data from the grid points. Therefore, seasonal and annual rainfall maps were created to illustrate the rainfall variations within the Wolaita Zone.

## 3. Results and Discussion

### 3.1. Variability and Trends of Rainfall

#### 3.1.1. Variability of Rainfall

The mean annual and seasonal rainfall variability in the Wolaita Zone is presented in Table 1. The research area experiences bimodal rainfall and receives high amounts of rainfall during the Kiremt season, which is the main rainy season. The Belg rainfall contributes a small amount of total rainfall. The mean annual rainfall in the study area was 1157.59 mm. However, the seasonal rainfall variability was highest in the Belg season and lowest in the Kiremt season in the Wolaita Zone. The Belg rainfall is much more variable than the summer (Kiremt) rainfall distribution variation. The Kiremt rainfall distribution is more variable than the annual rainfall distribution variation across the study area.

**Table 1.** Mean (annual and seasonal) rainfall and coefficient of variation.

Stations	Annual		Belg		Kiremt	
	Mean	CV (%)	Mean	CV (%)	Mean	CV (%)
Abaya	766.53	22.77	306.41	32.88	309.76	37.08
Areka	1377.02	27.12	475.07	36.55	700.44	32.66
Bilate	817.51	23.84	315.66	38.79	315.99	29.80
Boditischool	1224.33	15.82	470.44	30.21	558.05	22.68
Bombe	1374.79	29.65	497.39	33.64	687.03	40.87
Gesuba	1007.49	27.11	398.10	31.34	429.67	36.62
Halale	1230.21	27.48	465.17	30.62	551.26	41.88
Humbotebela	1110.59	24.22	375.37	28.68	530.64	40.70
Shanto	1124.24	16.59	426.53	33.26	531.82	23.10

Stations	Annual		Belg		Kiremt	
	Mean	CV (%)	Mean	CV (%)	Mean	CV (%)
Wolaita sodo	1332.08	16.92	472.77	28.51	635.91	25.13

### 3.1.2. Standardized Rainfall Anomaly Index

The standard rainfall anomalies were computed and the result indicated that there were positive and negative anomalies, which implied the presence of inter-annual rainfall variability across the observed time series. In the Annual standardized rainfall the highest positive anomaly (+2.13) was observed in the year 2020 and the lowest negative anomaly (-1.40) was observed in the year 1991. In the Belg season standardized rainfall the highest positive anomaly (+2.97) was observed in the year 2019 and the lowest negative anomaly (-1.33) was observed in the year 2015. In the Kiremt season standardized rainfall the highest positive anomaly (+2.15) and the lowest negative anomaly (-1.13) was observed in the year

1991. According to the drought assessment method by from seventeen dry years: one severe (2015), six moderate (1999, 2008, 2009, 2011, 2017 and 2019) and no drought (1992, 1994, 2000, 2001, 2002, 2003 2004, 2006 and 2014) dry years were identified in the belg season. During Kiremt season from fourteen dry years: five severe drought (1991, 1993, 2002, 2004 and 2016), four moderate (1991, 1995, 1997 and 1999) and no drought (1992, 2006, 2015, 2017 and 2018) dry years were identified in the kiremt season and during annual from fifteen dry years: one (1991), six moderate (1992, 1993, 2002, 2004, 2015 and 2017) and no drought (1994, 1995, 2001, 2006, 2009, 2011 and 2016) dry years were identified in the annually.

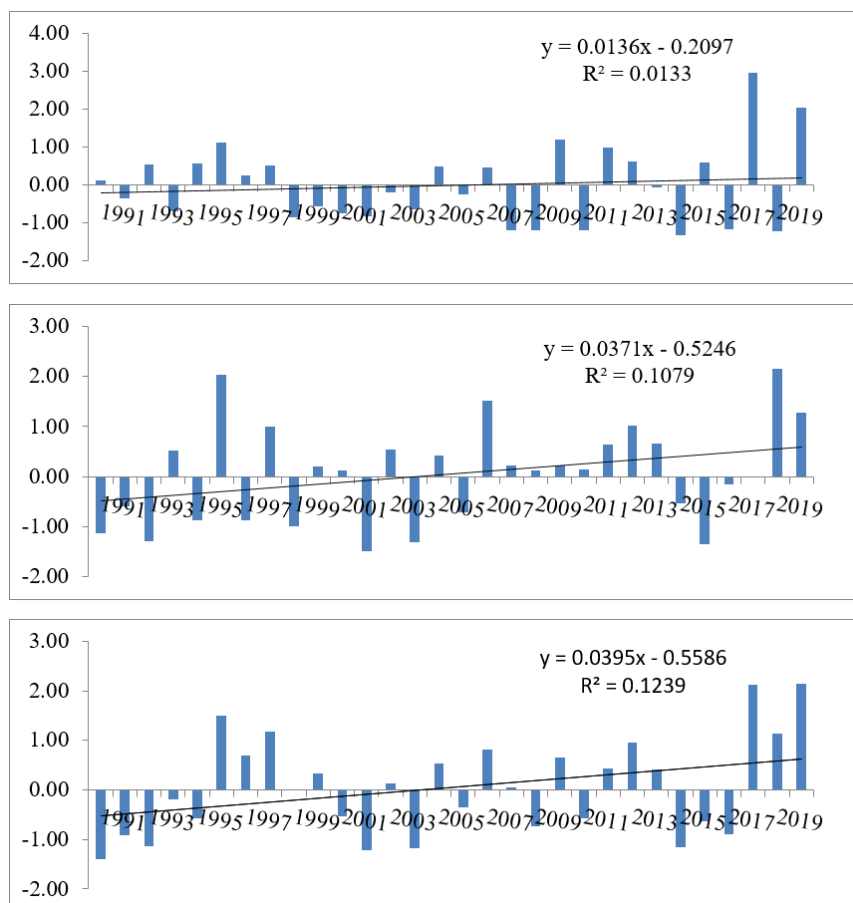


Figure 2. Standardized Belg, Kiremt and Annual Anomalies.

### 3.1.3. Trends of Rainfall

The Kiremt and annual rainfall data indicate a declining trend at three and two stations, respectively, even though the Kiremt rainfall data are not statistically significant except at the Halale and Shanto stations, where there is a statistically significant ( $P < 0.05$ ) reduction in the Kiremt rainfall trend, as

shown in Table 2. However, Halale and Shanto registered significant increases in the annual rainfall of the Wolaita Zone. The Belg season rainfall shows no statistically significant increasing trend ( $P < 0.05$ ) at any of the 15 stations. Generally, the direction and magnitude of the seasonal rainfall trend were not uniform across the different stations.

**Table 2.** Mann–Kendall ( $Z$ ) and Sen's slope ( $Q$ ) trend test (mm/year) results for the annual, Belg, and Kiremt rainfall at the selected stations in the Wolaita Zone, southern Ethiopia.

Stations	Annual			Belg-season			Kiremt-season		
	Z	Q	p value	Z	Q	p value	Z	Q	p value
Abaya	0.19	8.24	0.14	-0.02	-0.38	0.92	0.20	5.47	0.11
Areka	0.03	0.40	0.80	-0.13	-2.67	0.32	0.18	3.56	0.16
Bilate	0.14	6.47	0.30	0.15	2.32	0.25	0.14	3.17	0.27
Boditischool	-0.23	-12.56	0.07	-0.23	-5.88	0.07	0.25	9.91	0.05
Bombe	0.23	15.51	0.07	0.03	0.50	0.80	-0.06	9.91	0.66
Gesuba	0.16	5.43	0.21	0.02	0.55	0.87	0.23	3.19	0.07
Halale	0.28	8.76	0.03	0.06	1.48	0.64	0.26	4.20	0.04
Humbotebela	0.20	6.95	0.13	-0.18	-2.82	0.17	0.18	6.59	0.15
Shanto	0.39	21.25	0.00	0.01	0.44	0.97	0.47	16.95	0.00
Wolaita sodo	0.14	4.54	0.26	0.06	1.14	0.67	0.10	2.02	0.46

Bold values indicate a significance level of  $P < 0.05$ .

### 3.2. Spatial Distributions of Season and Annual Rainfall

Figure 3 shows the spatial distribution of the seasonal and annual rainfall in the Wolaita Zone. In the Belg season, the lowland area of the Wolaita Zone is dominated by decreasing rainfall. However, significant decreasing and increasing rainfall trends occurred in the highland area of the Wolaita Zone. The remaining part of the Wolaita Zone is dominated by an increasing rainfall distribution. The spatial distribution of Belg rainfall shows that the rainfall of the lowland area of the

Wolaita Zone is less than the average rainfall value, whereas the highland area of the Wolaita Zone receives more rainfall than the average. The rainfall in the Kiremt season shows a dominance-increasing distribution in most parts of the Wolaita Zone. In general, some parts of the lowland area of the Wolaita Zone significantly decrease rainfall distributions, whereas the highland area of the Wolaita Zone presents significantly increasing rainfall distributions. The spatial distribution pattern of annual rainfall reflects the combined effect of seasonal rainfall. The rainfall distribution decreases in the lowland area of the Wolaita Zone. The remaining parts of the Wolaita Zone show increasing rainfall distributions.

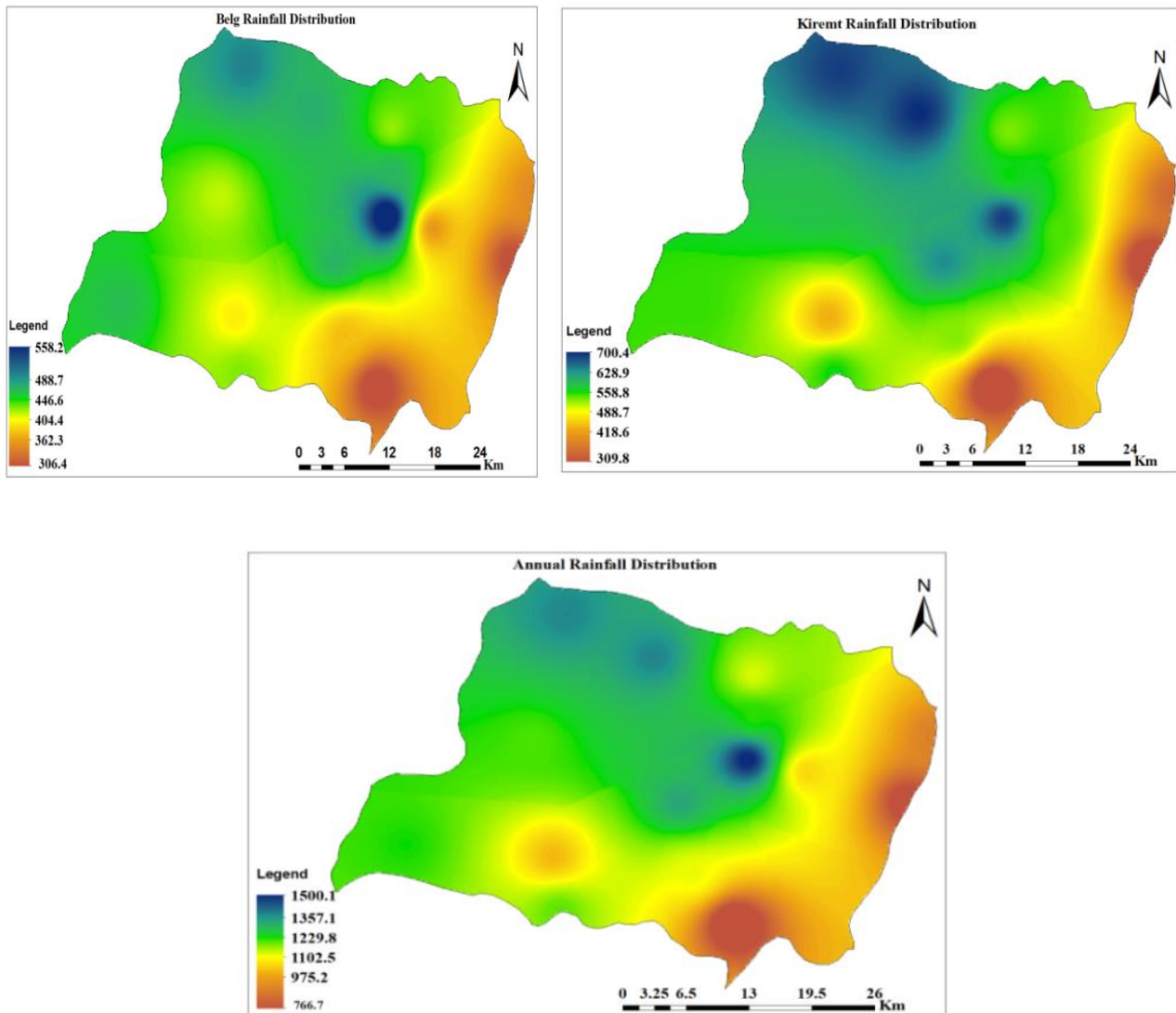


Figure 3. Spatial distribution of annual and seasonal rainfall.

#### 4. Conclusion

This paper examined the spatiotemporal variability and trend of annual and seasonal rainfall in the Wolaita Zone. Rainfall is highly variable across the Belg season. Rainfall distribution during the Kiremt season is moderately variable and shows a significant increase in trend. A mean rainfall of the study area from 1991 to 2020 was received from highest to lowest total rainfall, 910.3 mm to 1465.9 mm, respectively. There is significant rainfall variability during seasonal timescales than annual timescales. Spatially, rainfall distribution decreases in the southern, southwestern, southeastern, and eastern parts of the Wolaita Zone. The remaining parts of the Wolaita Zone show increasing rainfall distributions. Rainfall is highly variable in intensity and distribution, both spatially and temporally. Some of the adverse effects of extreme rainfall here are surface and groundwater scarcity, crop losses, and

lack of feed for livestock. Therefore, communities and local actors need to devise appropriate adaptation strategies that can strengthen their capacity during and post-disaster periods and absorb the adverse effects. The decision-maker needs to make informed decisions by taking into account local variability and the degree of climate-related risk.

#### Abbreviations

CV	Coefficient of Variability
ENACTS	Enhanced National Climate Services
IDW	Inverse Distance Weighted
MK	Mann–Kendall
Q	Sen’s Slope
SRA	Standardized Rainfall Anomaly
WZFEED	Wolaita Zone Finance and Economic Development Department

## Author Contributions

Adugna Arba is the sole author. The author read and approved the final manuscript.

## Conflicts of Interest

The author declares no conflicts of interest.

## References

- [1] Agnew, C. T., & Chappell, A. (1999). Drought in the Sahel. *GeoJournal*, 48(4), 299-311. <https://doi.org/10.1023/A:1007059403077>
- [2] Birch, E. L. (2014). A Review of “Climate Change 2014: Impacts, Adaptation, and Vulnerability” and “Climate Change 2014: Mitigation of Climate Change.” *Journal of the American Planning Association*, 80(2), 184-185. <https://doi.org/10.1080/01944363.2014.954464>
- [3] Degefu, M. A., Rowell, D. P., & Bewket, W. (2017). Teleconnections between Ethiopian rainfall variability and global SSTs: observations and methods for model evaluation. *Meteorology and Atmospheric Physics*, 129(2), 173-186. <https://doi.org/10.1007/s00703-016-0466-9>
- [4] Dinku, T., Thomson, M. C., Cousin, R., del Corral, J., Ceccato, P., Hansen, J., & Connor, S. J. (2018). Enhancing National Climate Services (ENACTS) for development in Africa. *Climate and Development*, 10(7), 664-672. <https://doi.org/10.1080/17565529.2017.1405784>
- [5] Esayas, B., Simane, B., Teferi, E., Ongoma, V., & Tefera, N. (2019). Climate Variability and Farmers’ Perception in Southern Ethiopia. *Advances in Meteorology*, 2019. <https://doi.org/10.1155/2019/7341465>
- [6] Finance, W. Z. (n.d.). Economic Development Department (2017). *Wolaita Zone Finance and Economic Development Department Data Collection, Organization and Dissemination Work Process Annual Abstract, Wolaita Soddo, SNNPRS, Ethiopia*.
- [7] Gautam, M., & Singh, A. K. (2015). Impact of climate change on water resources. *Climate Change Modelling, Planning and Policy for Agriculture*, 2(1), 219-231. [https://doi.org/10.1007/978-81-322-2157-9\\_21](https://doi.org/10.1007/978-81-322-2157-9_21)
- [8] Harka, A. E., Jilo, N. B., & Behulu, F. (2021). Spatial-temporal rainfall trend and variability assessment in the Upper Wabe Shebelle River Basin, Ethiopia: Application of innovative trend analysis method. *Journal of Hydrology: Regional Studies*, 37 (September), 100915. <https://doi.org/10.1016/j.ejrh.2021.100915>
- [9] Indeje, M., Semazzi, F. H. M., & Ogallo, L. J. (2000). ENSO signals in East African rainfall seasons. *International Journal of Climatology*, 20(1), 19-46. [https://doi.org/10.1002/\(SICI\)1097-0088\(200001\)20:1<19::AID-JOC449>3.0.CO;2-0](https://doi.org/10.1002/(SICI)1097-0088(200001)20:1<19::AID-JOC449>3.0.CO;2-0)
- [10] Jain, S. K., & Kumar, V. (2012). Trend analysis of rainfall and temperature data for India. *Current Science*, 102(1), 37-49.
- [11] Korecha, D., & Barnston, A. G. (2007). Predictability of June-September rainfall in Ethiopia. *Monthly Weather Review*, 135(2), 628-650. <https://doi.org/10.1175/MWR3304.1>
- [12] Mann, H. B. (1945). Non-parametric test against trend. *Econometrica* 13, 245-259. *Search In*.
- [13] Mondal, A., Kundu, S., & Mukhopadhyay, A. (2012). *Case Study rainfall trend analysis by mann-kendall test : a case study of north-eastern part of cuttack district, Orissa School of Oceanographic Studies, Jadavpur University, Kolkata-700032 \* Author for Correspondence Case Study Trend Analysis*. 2(1), 70-78.
- [14] Moshinsky, M. (1959). Transformation brackets for harmonic oscillator functions. *Nuclear Physics*, 13(1), 104-116.
- [15] Nicholson, S. E. (1985). American Meteorological Society Author (s): Sharon E. Nicholson Source : *Journal of Climate and Applied Meteorology*, Vol. 24, No. 12 (December 1985), pp. Published by : American Meteorological Society Stable URL : <https://www.jstor.org/stable/26> *Climate and Applied Meteorology*, 24(12), 1388-1391.
- [16] Sen, P. K. (1968). Estimates of the Regression Coefficient Based on Kendall ’ s Tau Author (s): Pranab Kumar Sen Source : *Journal of the American Statistical Association*, Vol. 63, No. 324 (Dec., 1968), pp. Published by : Taylor & Francis, Ltd. on behalf of the A. *Journal of the American Statistical Association*, 63(324), 1379-1389. <https://www.jstor.org/stable/2285891>
- [17] Solomon, S. D. (2007). Contribution of Working Group I to the fourth assessment report of the Intergovernmental Panel on Climate Change 2007. (*No Title*).
- [18] Theil, H. (1950). A rank-invariant method of linear and polynomial regression analysis, Part I. *Proceedings of the Royal Netherlands Academy of Sciences*, 53, 386-392.
- [19] Wasihun, G., & Desu, A. (2021). Trend of cereal crops production area and productivity, in Ethiopia. *Journal of Cereals and Oilseeds*, 12(1), 9-17. <https://doi.org/10.5897/jco2020.0206>
- [20] Weldegerima, T. M., Zeleke, T. T., Birhanu, B. S., Zaitchik, B. F., & Fetene, Z. A. (2018). Analysis of Rainfall Trends and Its Relationship with SST Signals in the Lake Tana Basin, Ethiopia. *Advances in Meteorology*, 2018. <https://doi.org/10.1155/2018/5869010>
- [21] WMO, W. M. O. (1988). Analyzing long time series of hydrological data with respect to climate variability. *Geneva: WMO Secretariat*.
- [22] Yadav, R., Tripathi, S. K., Pranuthi, G., & Dubey, S. K. (2014). Trend analysis by Mann-Kendall test for precipitation and temperature for thirteen districts of Uttarakhand. *Journal of Agrometeorology*, 16(2), 164-171.